BOND GRAPH METHODS APPLIED TO THE VIBRATION CONTROL OF A LARGE AIRCRAFT WING

Donald Margolis
University of California
Davis, California

ABSTRACT

Bond graphs of finite modal representations of one-dimensional continuous systems are developed. Emphasis is placed on "one-dimensional, soft" structures such as large aircraft wings or the wings of vertical take off and landing (VTOL) vehicles. The displacement (and internal stress) control of a large aircraft wing is demonstrated through simulation on a digital computer.

NOMENCLATURE

A	area
b	damping constant
C	bond graph compliance
C_v	vertical support compliance
C_τ	torsional support compliance
d	nondimensional damping constant
EI	section modulus
F	force
F_{c_1}	force at control location 1
F_{c_2}	force at control location 2
F_{e_1}	force at engine location 1
F_{e_2}	force at engine location 2
g	acceleration of gravity
I	bond graph inertia
ℓ_w	wing length
M	moment
m_r	r^{th} modal mass
R	bond graph resistance
t	time
w	transverse wing deflection
x	position
x_{c_1}	position of control 1
x_{c_2}	position of control 2
x_{e_1}	position of engine 1
x_{e_2}	position of engine 2
Y_r	r^{th} mode shape
δ	dirac delta function
η_r	r^{th} modal time function
ξ	modal damping ratio
ρ	mass density
ω_r	r^{th} modal frequency

INTRODUCTION

Control of the vibration of continuous systems finds importance in applications as varied as wings of large aircraft to multistory buildings. In fact, it has just recently been made public that the C5A cargo transport has severe wing fatigue problems due to large wing deflections during landing and take-off. This problem cuts the useful life of the plane by 1/3. Couple this with a cost override of a factor of 2, and the C5A currently costs six times its original estimate. If these wing vibrations could be controlled inexpensively, great savings would result.

One of the major problems in controlling the vibration of soft, cantilever structures, such as wings or tall buildings, is the difficulty of applying the control force at other than the attached end of the structure. In general, a force actuator must be attached to "ground" in order to generate a restoring force. This is, of course, impossible in the case of a wing tip of a landing aircraft or the upper floors of a multistory building.

An additional problem in the closed loop control of inherently distributed systems is that instability is easily generated by sensing motion at one location (such as the wing tip) and applying forces at another (such as near the attachment point). This point will be demonstrated shortly. This stability problem is alleviated if the motion and control force are measured and applied at the same location. This fact will also be demonstrated shortly.

It is possible to generate control forces at any location on the structure without attachment to "ground". In the case of jet aircraft wings, ducting some of the engine thrust to the proper locations is a means of providing forces at virtually any location. For other structures where momentum flux devices are not practical, inertia force actuators can be employed. By simply accelerating a mass according to some control policy virtually any force-time history can be generated.

The question of required magnitude of control forces, frequency response, and necessary power for controller operation is answered through modeling and simulation of the systems involved. This is a cheap method of determining the practicality of a proposed solution and is an important step in the design process.

In what follows, bond graph models are developed for the modal dynamic behavior of a large aircraft wing (such as a C5A). Simple closed loop control is then applied and shown to be a feasible solution to the C5A wing deflection problem. The bond graph modeling technique is not developed in any detail here. It is completely documented in Reference [1].

WING MODEL

The physical configuration of the wing is shown in Figure 1. In this example provision is made for two engines suspended from the wing and for the application of control forces at two general locations. The wing appears cantilevered at the left; however, in the formulation to follow any dynamics associated with the landing gear, deflection of the fuselage, etc. will be incorporated into the left support.

For demonstration of control applications, the wing can be reasonably well modeled as a uniform Bernoulli-Euler beam. In Figure 2 this beam is shown with all external reactions from the engines, control, and left support in their assumed positive directions. At this point, the classical modal approach [2] is used to reduce the governing partial differential equation to an infinite set of uncoupled total differential equations. As will be seen, the uncoupled modal equations lend themselves to direct formulation into a bond graph model.

Assuming the forces and moment of Figure 2 are applied at discrete locations, the governing partial differential equation in terms of the transverse beam displacement, w(x,t), becomes

$$EI \frac{\partial^4 w}{\partial x^4} + \rho A \frac{\partial^2 w}{\partial t^2} = F\,\delta(x) + F_{e_1}\,\delta(x - x_{e_1}) + F_{e_2}\,\delta(x - x_{e_2}) + F_{c_1}\,\delta(x - x_{c_1}) + F_{c_2}\,\delta(x - x_{c_2}) + M\frac{d}{dx}\delta(x) \quad (1)$$

Following modal analysis procedure, the homogeneous form of equation (1) is solved with the assumed solution

$$w(x,t) = Y(x) \cdot \eta(t) \quad (2)$$

This yields an equation for the mode shapes, Y(x), as

$$EI \frac{d^4 Y}{dx^4} = \rho A \omega^2 Y \quad (3)$$

Equation (3) is solved, subject to proper boundary conditions, to yield equations for the natural frequencies, ω_r^2, and corresponding mode shapes, $Y_r(x)$.

The question of "proper boundary conditions" subjects the modal approach to perhaps more criticism than any other aspect. It is generally believed that each time a new boundary condition is introduced the problem must be entirely reformulated. This is strictly true if any fixed displacement (or geometric) boundary conditions are imposed. Certainly the mode shapes associated with a zero deflection boundary condition can add up to nothing different from zero at the boundary even if a change to a zero force condition is desired. However, the mode shapes associated with force free boundary conditions are perfectly capable of adding to zero velocity (or displacement) should a fixed boundary condition be imposed. Karnopp [3] has shown that force free normal modes and frequencies produce excellent prediction of the natural frequencies associated with the same system but with fixed boundary conditions. Some accuracy is lost at the higher frequencies and thus if boundary conditions are to be changed then one or two additional modes should be retained over and above what the frequency content of the forcing would normally dictate.

The principal drawback to using the force-free normal modes is that they are the most difficult mode shapes to compute. However, they need only be computed one time to provide for solutions to a vast variety of system geometries and boundary conditions.

In order to maintain generality and allow for dynamic behavior at the attached end of the wing, the force-free (no shear and no moment) normal modes associated with equation (3) will be used. For the Bernoulli-Euler model, these mode shapes and frequencies can be derived analytically [2] and thus will not be derived here. It should be noted that the first two normal modes, $Y_0(x)$ and $Y_1(x)$, correspond to the rigid body translation and rotation of the beam.

To complete the modal analysis formalism, the complete equation (1) is solved with the assumed solution

$$w(x,t) = \sum_{r=0}^{\infty} Y_r(x) \cdot \eta_r(t) \quad (4)$$

where $Y_r(x)$ are the force-free normal modes. By substituting (4) into (1) and the result mutiplied by $Y_s(x)$ and integrated over the domain x = 0 to x = ℓ_w, decoupled modal equations result.

$$m_r \ddot{\eta}_r + m_r \omega_r^2 \eta_r = F\,Y_r(0) + F_{e_1} Y_r(x_{e_1}) + F_{e_2} Y_r(x_{e_2}) + F_{c_1} Y_r(x_{c_1}) + F_{c_2} Y_r(x_{c_2}) + M\frac{d}{dx} Y_r(0) \quad (5)$$

where

$$m_r = \int_0^{\ell_w} \rho A Y_r^2 \, dx \quad (6)$$

is the modal mass and, unfortunately, must be computed. For a Bernoulli-Euler model, m_r can be computed analytically.

Equations (5) are directly amenable to bond graph representation. The left side of (5) is an infinite set of uncoupled oscillators of mass, m_r, and stiffness, $m_r \omega_r^2$. In a bond graph these oscillators become inertia and compliance elements attached to force summing 1-junctions. The right side of (5) are the actual applied forces multiplied by appropriate modifying constants. These constants, or mode participation factors, are represented by transformers in the system bond graph. Examples of bond graphs applied to modal dynamics can be found in References [1], [3], and [4].

Figure 3 is the bond graph representation of the wing configuration of Figure 1. Five normal modes have been retained in this model. Reference [5] indicates that five modes are sufficient to compute moments to within 5% accuracy and even better accuracy in computing displacements. The applied forces and moment of Figure 2 are indicated on appropriate bonds in Figure 3.

The I ⟵ and C ⟵ elements emanating from the 1-junctions are the oscillators associated with each normal mode. Each I element equals one modal mass, m_r, while each C element equals the inverse of one modal stiffness, $m_r \omega_r^2$. The first two 1-junctions have only I⟵ elements attached. This is due to the first two modes being the rigid body translation and rotation of wing and are thus nonoscillatory. Also, resistance elements have been incorporated into the dynamic modes. This provides for modal damping and is adjusted, in this example, to yield a damping ratio, ξ, of 0.02 for each mode.

The forcing for each mode is a result of the applied forces and moment acting through appropriate mode participation factors (TF's). The TF moduli are nothing more than the mode shapes (and slope in the case of M) evaluated at the location of the applied effort. The applied forces act on 0-junctions in order to sum the modal velocities to yield the actual velocities at each force location.

Also shown in Figure 3 are the causal strokes (perpendicular lines at the end of each bond) which totally determine the number of equations and independent variables required in the formulation. In order to maintain integral causality throughout the bond graph it is necessary to

specify the applied forces (and moment) as inputs to the modal dynamics while the modes, in turn, determine the velocities (or angular velocity) as outputs. This is accomplished by using force (or moment) generators--compliance elements--on the external bonds. Thus, on the left of Figure 3, the vertical support stiffness is represented by the compliance, C_v, while the rotational stiffness is given by C_T. As these compliances are made small, a true cantilever support is approached. The effect of vertical dynamics of the aircraft on the wing support can be incorporated into the C_v element.

The engines are modeled by the engine inertia, I_e, engine weight, S_e, and pilon compliance C_e. The engines can be attached at any location along the wing desired. Finally, the control forces are specified by some control law and will be discussed next.

STABILITY OF THE CONTROL ACTION

As mentioned previously, an inherent stability problem exists whenever a control action is applied at one location of a distributed system and that control action is a function of the motion at another location. This can be demonstrated analytically as follows.

Consider the modal equations (5) with only one control force, F_c, acting at position x_c. Thus

$$m_r \ddot{\eta}_r + m_r \omega_r^2 \eta_r = F_c(x_c)\, Y_r(x_c) \tag{7}$$

Assume that F_c is proportional to the velocity, $\dot{w}$, at some other location, x_s, i.e., let

$$F_c(x_c) = -b\dot{w}(x_s) \tag{8}$$

but

$$\dot{w}(x_s) = \sum_{r=0}^{\infty} Y_r(x_s)\, \dot{\eta}_r(t) \ . \tag{9}$$

Thus

$$F_c(x_c) = -b \sum_{r=0}^{\infty} Y_r(x_s)\, \dot{\eta}_r(t) \tag{10}$$

Substituting (10) into (7) generates

$$\begin{aligned}
&m_1 \ddot{\eta}_1 + m_1 \omega_1^2 \eta_1 + b\, Y_1(x_c)\, Y_1(x_s)\, \dot{\eta}_1 + b\, Y_1(x_c)\, Y_2(x_s)\, \dot{\eta}_2 \\
&+ b\, Y_1(x_c)\, Y_3(x_s)\, \dot{\eta}_3 + - - - = 0 \\
&m_2 \ddot{\eta}_2 + m_2 \omega_2^2 \eta_2 + b\, Y_2(x_c)\, Y_1(x_s)\, \dot{\eta}_1 + b\, Y_2(x_c)\, Y_2(x_s)\, \dot{\eta}_2 \\
&+ b\, Y_2(x_c)\, Y_3(x_s)\, \dot{\eta}_3 + - - - = 0 \\
&\quad \cdot \\
&\quad \cdot \\
&\quad \cdot \\
&m_n \ddot{\eta}_n + m_n \omega_n^2 \eta_n + b\, Y_n(x_c)\, Y_1(x_s)\, \dot{\eta}_1 + b\, Y_n(x_c)\, Y_2(x_s)\, \dot{\eta}_2 \\
&+ b\, Y_n(x_c)\, Y_3(x_s)\, \dot{\eta}_3 + - - - = 0
\end{aligned} \tag{11}$$

Do equations (11) represent a stable closed loop system? For a finite number of retained modes, Routh's criterion or Liapunov stability could be applied; however, it can simply be stated that if x_c and x_s are selected such that equations (11) are stable, then x_c and/or x_s could be selected such that the product $Y_i(x_c)\, Y_j(x_s)$ would change sign and produce an unstable system. In addition, even if the controller is stable for the number of modes retained in the actual system, if more modes are excited than anticipated, instability could result.

If the control action and system motion are applied and sensed at the same location ($x_c = x_s$), the stability is insured. This, too, can be demonstrated analytically; however, heuristically, if the control force is proportional to the negative of the velocity at the force location, then the control action is identical to attaching a damper at that location. The damper will always dissipate energy and cannot cause instability. Thus for soft, nonrigid-bodylike structures it is desirable to sense motions and apply control actions at the same location.

For the five mode representation of a large aircraft wing shown in Figure 3, two stable control actions will be demonstrated. The first is to apply a restoring force proportional to transverse velocity at some location along the wing. This could be accomplished by ducting "thrust" from the aircraft engines to the control locations. The second is to provide a constant restoring "thrust" at the control locations, turning the control action "off" for wing tip velocities below some arbitrary level. The second approach would be much simpler with regard to design of an actual system. Optimal control techniques could also be incorporated as demonstrated in Reference [6].

RESULTS

Typical parameter values for the C5A wing were supplied through personal correspondence with the Lockheed-Georgia Company. Obviously, the wing is not a uniform Bernoulli-Euler beam and the parameter values listed below are average values where necessary.

ℓ_w, wing length = 100 ft

EI, section modulus = 3.25×10^9 $Lb_f\ ft^2$

ρAg, weight/unit length = 1182 Lb_f/ft
(typical for 50% fuel remaining)

Engine weight = 10917 Lb_f each

x_{e_1}, x_{e_2}, engine locations = 40 ft, 60 ft

Engine support stiffness = 1.35×10^6 Lb_f/ft

Using methods described in [1], the 26 governing state space equations were derived directly from the bond graph. These equations were solved numerically using the digital computer for the different control options described previously. For all results that follow a vertical landing velocity of 5 ft/sec is assumed. This velocity is typical of about 5% of the landings of the C5A. These results are characteristic of the type of parameter studies which could be used fruitfully in the design process.

Figure 4 shows the predicted wing configuration for maximum tip deflection, nondimensionalized with respect to wing length. The engine locations are indicated, and no external control has been supplied. The response is primarily "first-mode" in this configuration with a tip deflection of 2.35 ft (28"). The actual tip deflection as reported by the Lockheed-Georgia Company for a vertical landing velocity of 5.3 ft/s is 31 inches. From Figure 5, the period of oscillation for the uncontrolled wing is approximately 1.6 s. The Lockheed-Georgia Company reports a period of 1.35 s. Comparing the predicted and actual deflection and frequency results, it is felt that the uniform Bernoulli-Euler beam model is reasonable at least for comparative parametric studies.

Figure 5 shows the wing tip deflection-time history for various control actions and parameters. The d-values are based on an equivalent second order system of mass equal to the total system mass and natural frequency commensurate with the uncontrolled period. It should be noticed from the uncontrolled deflection curve that higher mode effects are definitely present. Also, strongly coupled to Figure 5 is Figure 6 in which the maximum moments at the midsection of the wing are listed for the various control actions. These results are normalized with respect to the maximum midsection moment occuring in the uncontrolled case.

Figure 6 also lists the average horsepower requirement for implementation of each control action.

Figures 5 and 6 vividly demonstrate the desirability of control for the C5A wing. For tip control only, using a "linear damper" control action, dramatic decreases in deflection are accomplished requiring only 50 to 60 HP to implement the control action. Interestingly enough, the minimum midsection moment does not occur for the control action providing minimum deflection. Instead, as the feedback constant is increased, the maximum moment first decreases and then increases past d = 0.13. The minimum midsection moment is 34% less than the uncontrolled case.

For control at both the wing tip and midpoint using equal feedback constants corresponding to d = 0.13, the deflection history is hardly different than for tip control only using the same d. However the effective extra support at the midpoint reduced the maximum moment still further to 43% less than the uncontrolled case. The power expenditure remained virtually unchanged.

Finally, one case of tip control using a "constant thrust" control action is demonstrated in Figure 5. This simple control action still provides substantial deflection decreases as well as 20% reduction in maximum midsection moment.

The results and parameter studies discussed here could be carried out endlessly. Sophisticated optimization could be employed and the data correlated many different ways. It is not claimed that an exhaustive study has been presented; however, the utility and necessity of digital simulation in the design process has been demonstrated.

CONCLUSIONS

A bond graph model of the finite mode representation of a large aircraft wing has been developed. The model provides for dynamics at the wing-fuselage attachment as well as allowing for any engine location and engine support dynamics. The model also provides for two arbitrary control action locations.

Using typical wing parameters for a C5A wing, simulations were carried out for various control policies and various control action locations. The results vividly demonstrate the practicality of using active force generators for the vibration control of the C5A wing.

REFERENCES

1. Karnopp, Dean, and Rosenberg, Ronald, System Dynamics: A Unified Approach, John Wiley and Sons, New York, 1975.

2. Meirovitch, Leonard, Analytical Methods in Vibrations, Macmillan, New York, 1967.

3. Karnopp, D. C., "Computer Representation of Continuous Vibratory Systems Using Normal Modes and Bond Graph Techniques", Simulation, Vol. 10, No. 3, March 1968.

4. Margolis, D. L., "Finite Mode Bond Graph Representation of Vehicle-Guideway Interaction Problems", submitted for publication in the Journal of the Franklin Institute.

5. Smith, C. C., and Wormley, D. N., "Response of Continuous Periodically Supported Guideway Beams to Traveling Vehicle Loads", Journal of Dynamic Systems, Measurement, and Control, Trans. ASME, Vol. 97, Series G, No. 1, March 1975.

6. Van De Vegte, J., and Hladun, A. R., "Design of Optimal Passive Beam Vibration Controls by Optimal Control Techniques", ASME Journal of Dynamic Systems, Measurement, and Control, Vol. 95, Series G, p. 427, 1973.

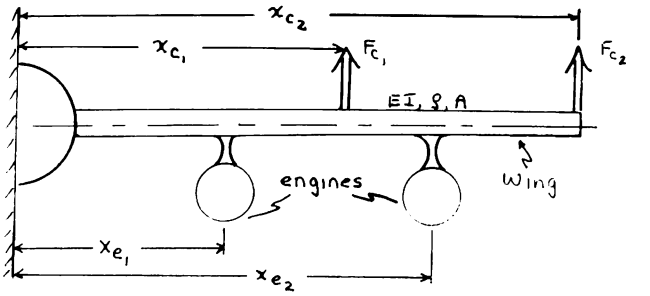

Figure 1 Physical Configuration of Wing

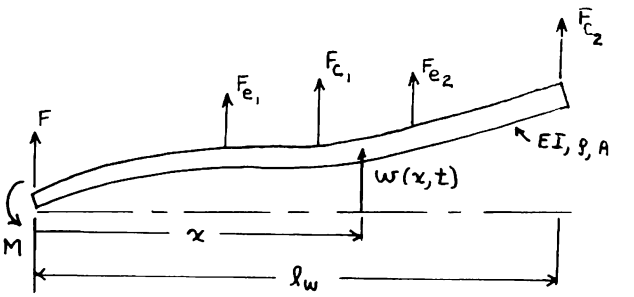

Figure 2 Beam Representation of the Wing

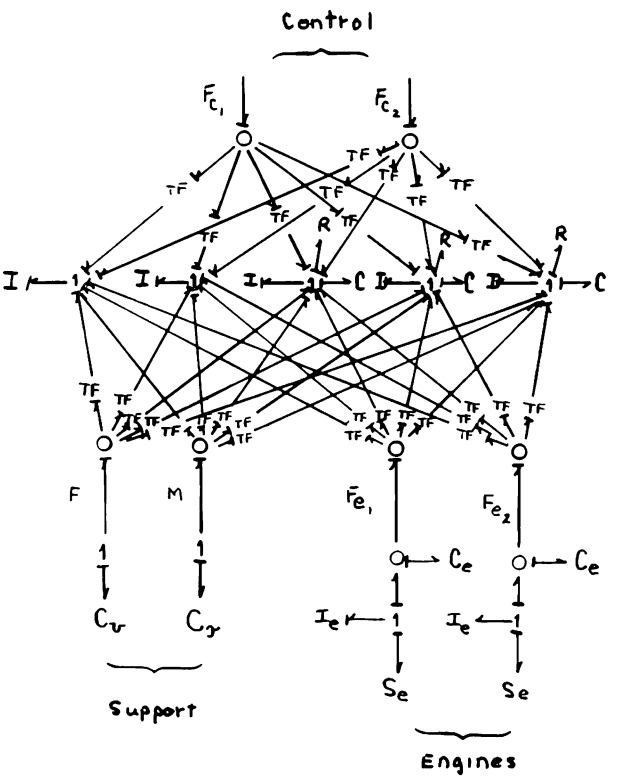

Figure 3 Bond Graph Model of Aircraft Wing

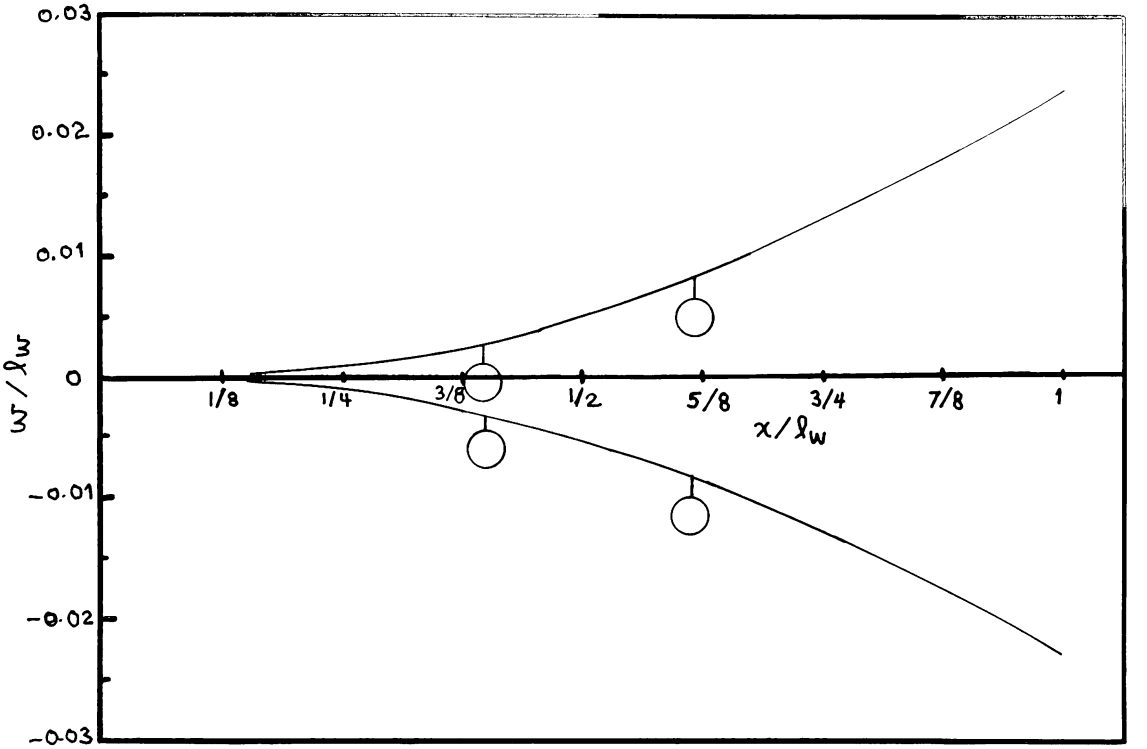

Figure 4 Wing Configuration for Maximum Tip Deflection

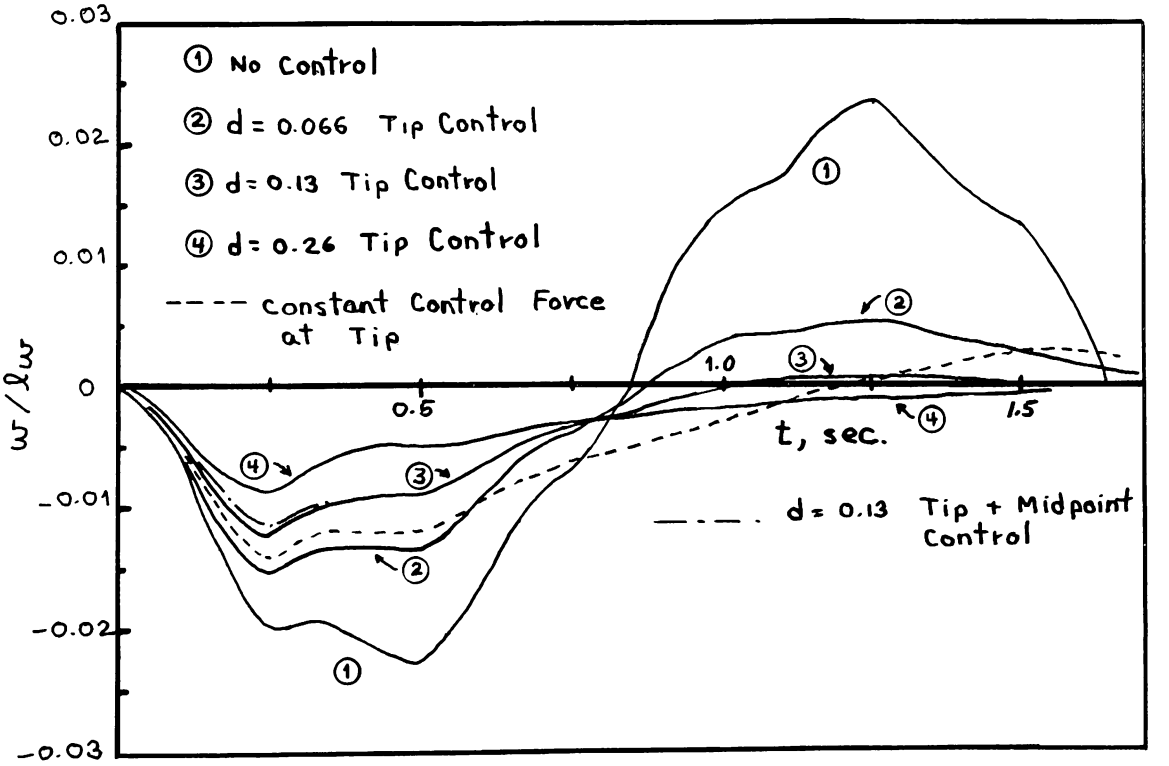

Figure 5 Tip Deflection vs Time for Various Control Actions

Control Action	Normalized Max. Moment	Average Horsepower
no control	1.0	0.0
d = 0.06c tip control	0.79	51.0
d = 0.13c tip control	0.66	56.4
d = 0.26c tip control	0.62	60.3
d = 0.52c tip control	0.74	64.5
constant force tip control	0.80	61.0
d = 0.13c tip & midpoint control	0.77	60.0

Figure 6 Maximum Midsection Moments and Power Requirement for Various Control Actions